Annual Technical Report
Phase II
1 February 2006 to 31 March 2007
NREL Subcontract No. XXL-5-44205-09
Principal Investigator: George A. Williams
Organization: University of Utah
Co-:Principal Investigator: P. Craig Taylor
Organization: Colorado School of Mines

Innovative Characterization of Amorphous and Thin-Film Silicon for Improved Module Performance

I. Introduction

Research results during Phase II of NREL Subcontract XXL-5-44205-09 are reported. During this phase we continued our collaborations with United Solar Ovonics Corporation on defects that contribute to the Staebler-Wronski effect in modules made using a-Si:H and a-Si_xGe_{1-x}:H intrinsic layers. We performed NMR experiments on two samples in an attempt to confirm our earlier results on the metastable hydrogen doublet site at better signal-to-noise ratios. We are continuing our collaborations with NREL on defects generated in tritiated a-Si:H. Specifically, we have measured the growth of defects at 77 K and performed both isochronal and isothermal annealing at elevated temperatures. In addition, we have continued our studies of light soaking at 77 K to determine that the Staebler-Wronski effect does not saturate at this temperature but rather grows continuously just as occurs in the case of the tritium decay. Recently, we added a second sample at 77 K in which we are employing white diodes at 77 K as the light source as opposed to the standard infrared-filtered ELH lamp.

We have finished our NMR studies of samples from United Solar Ovonics, which were purposely made to contain large defect densities. In these samples, using both NMR and FTIR measurements, we have positively identified a hydrogen doublet as due to dihydride bonding sites. Finally, we have completed our collaborative studies with Professor D. A. Drabold and T. A. Abtew at the Ohio University on calculations of the hydrogen-hydrogen separation at silicon dihydride bonding sites in a-Si:H and their potential role in metastabilities.

In this Annual Technical Report for Phase II we describe our characterization of the silicon dihydride bonding sites in a-Si:H and present detailed measurements of the hydrogen-hydrogen separation at these sites. We also describe our theoretical calculations of the hydrogen-hydrogen separation to compare with the experimental results.

II. Silicon Dihydride Bonding Sites in a-Si:H

The implication of hydrogen in the Staebler-Wronski effect (SWE) in hydrogenated amorphous silicon (a-Si:H) has generated enormous interest in understanding the local bonding environments of the hydrogen. In particular, recent proton (^{1}H) nuclear magnetic resonance (NMR) experiments have linked a specific metastable, “paired” hydrogen site, in which the

hydrogen pair is separated by 2.3 ± 0.2 Å, to the SWE [1]. Silicon dihydride (SiH_2) is a possible candidate for this site since calculations using the conventional tetrahedral silicon structure give 2.4 Å as the hydrogen separation [2].

Hydrogen environments can be probed using ^{1}H NMR techniques because the hydrogen nucleus communicates with the environment through a variety of spin-mediated interactions. In a-Si:H, the dipole-dipole interaction between two protons dominates. For these magnetic dipole interactions, the strength depends strongly on the proton-proton separation. Exciting the system with radiation corresponding to the interaction strength causes the proton system to resonate thereby producing a detectable time varying signal. The resulting Fourier-transformed line shape yields details of the local hydrogen bonding configurations. For instance, by analysis of dipole broadened line shapes, it has been determined that in a-Si:H bonded hydrogen in the silicon hydride (SiH) configuration exists in both clustered and essentially randomly isolated environments [1].

The SiH_2 line shape exhibits a well-known form resulting from a dipole interaction between two protons. An analytic expression of the intensity of this so-called "Pake doublet" line shape can be expressed in terms of the coupling strength, and hence the proton-proton separation, *r*. It is therefore possible to extract the proton-proton separation by fitting simulated line shapes to the experimental data. This would suffice if the SiH_2 existed as an isolated species with a well-defined *r*. In the case where modulations to the local field exist, due to nearby hydrogen nuclei, the pure Pake doublet is broadened by an amount corresponding to the proximity and number of the nearby nuclei. This "isotropic" broadening effect, which is Guassian for clustered arrays [3], can be taken as a fitting parameter in subsequent simulations.

Broadening of the pure Pake doublet may also result from a distribution of proton-proton separations. It is known from scattering experiments that the nearest neighbor, Si-Si bond angles vary by ± 10° [4]. Thus it is natural to expect some distribution in *r* that will reflect the amorphous system. The distribution can also be used as a fitting parameter whereby the resulting broadened spectrum is a summation of Pake doublets.

Observation of SiH_2 in low defect density a-Si:H has eluded ^{1}H NMR experiments primarily for two reasons. The first reason is obvious: in device quality films the SiH_2 concentrations are usually below the threshold detection limit of conventional ^{1}H NMR (~ 10^{16} cm^{-3}). Moreover, SiH occurs in concentrations ~ 10^{21} cm^{-3} and therefore dominates the line shape in standard free induction decay (FID) experiments. This fact alone suggests that the FID experiments are insufficient for observing the low concentrations of SiH_2.

A more subtle reason for the lack of experimental observation of SiH_2 in a-Si:H derives from the line shape broadening effects discussed above. Isotropic broadening becomes a problem when it is of the same the magnitude as the resolved dipolar coupling. In this case the Pake doublet is unresolved since its defining features smear to form a nearly Guassian line shape. For instance, the un-broadened proton dipolar coupling in SiH_2 with r = 2.4 Å is 13.4 kHz [3]. The typical clustered hydrogen environment yields a Gaussian with ~ 25 kHz full width at half

maximum (denoted henceforth as σ). Thus there will be no resolved SiH_2 line shape if it exists in an environment that resembles the standard clustered array.

In the present study, we have used ^1H NMR to obtain the stable SiH_2 Pake doublet. Simulations of the Pake doublet for various choices of broadening effects were performed. We discuss the simulation details and relevant fitting parameters needed to replicate the experimental data.

The a-Si:H sample used in this study was made at United Solar Ovonics Corporation at high growth rate (5 Å/s). The film was grown on aluminum foil at a substrate temperature of 200 °C. Such samples contain higher defect densities ($\geq 10^{17}$ cm^{-3}) and are generally not suitable for device applications. Fourier transform infrared spectroscopy (FTIR) measurements show IR active modes at 900 cm^{-1} and 850 cm^{-1}, indicative of the scissor and wagging SiH_2 modes, respectively. The presence of these modes in the FTIR spectrum implies an SiH_2 concentration on the order of 10^{21} cm^{-3} – well above the observation threshold for NMR. For subsequent NMR measurements, the sample was prepared as a powder according to methods previously discussed [1].

For spectral simulations, we numerically compute the "powder pattern" using a method similar to that described by Slitcher [5]. The program was built in C++ using the pre-written functions of the GAMMA libraries [6]. For simulations requiring a distribution of *r*, we chose a Gaussian distribution where σ and mean separation, R_o, are the fitting parameters. Thus the full spectrum resulting from a distribution in *r* is the summation of individual powder patterns (whose weight depends on the distribution parameters).

Figure 1 shows the frequency domain spectrum of the experimentally obtained Pake doublet with two simulations superimposed. We obtain the experimental Pake doublet by Fourier transforming the time domain signal and subtracting the remaining molecular hydrogen signal. The Zeeman frequency (147.417 MHz) has been subtracted so that the spectral center occurs at 0 Hz. The solid line represents the experimental Pake doublet. For comparison we present the simulated Pake doublets for r = 1.8 Å (peaks at ± 15 kHz) and 2.4 Å (peaks at ± 7 kHz). These simulations are broadened by 1 kHz, but they do not include a distribution of distances. The areas have been normalized to equal that of the experimental data.

Figure 2 demonstrates, in frequency space, the separate effects of isotropic broadening by clustering and by a distribution in *r*. The top trace represents the unbroadened powder pattern for r = 1.8 Å. Below it, we present a spectrum broadened by 15 kHz (approximately 72% of the dipolar coupling). The bottom trace represents the powder pattern for a Gaussian distribution of *r* characterized by the parameters R_o = 1.8 Å, σ = 0.52 Å (30% of R_o). The bottom trace has been further broadened by 1 kHz. Similarities between the broadened spectra suggest that the set of simulation parameters replicating the data is not unique.

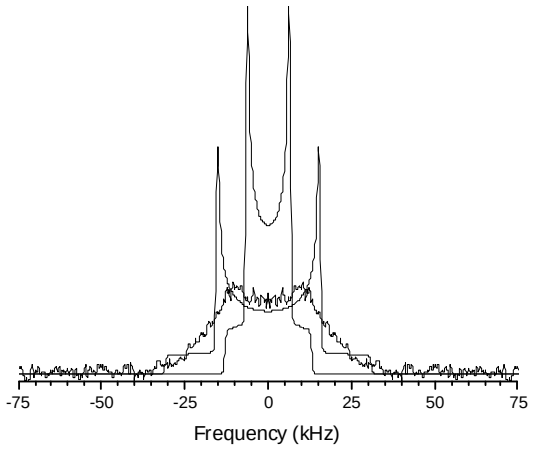

Figure 1. Frequency domain spectrum of the experimental Pake doublet with simulations for r = 1.8 Å (shoulder peaks at ± 15 kHz) and r = 2.4 Å (shoulder peaks at ± 7 kHz). The experimental data were obtained via a Fourier transform of the time domain data and subsequent subtraction of the molecular hydrogen signal. The Zeeman frequency (147.47 MHz) has been subtracted out so that the spectral center occurs at 0 Hz.

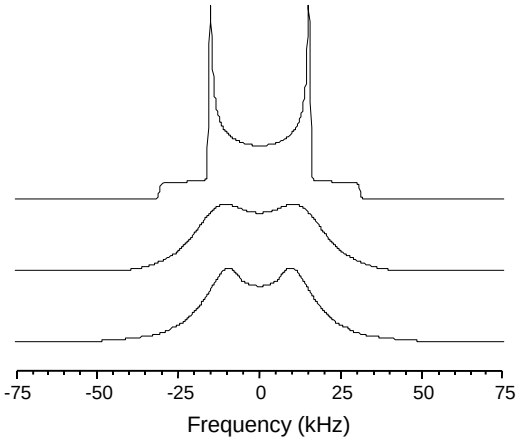

Figure 2. Broadening effects on the simulated Pake doublet for r = 1.8 Å. The top trace is a unique Pake doublet broadened by 1 kHz. The middle trace is the Pake doublet for r = 1.8 Å (no distribution) with 15 kHz isotropic broadening. The bottom trace represents the Pake doublet simulation for R_o = 1. 8 Å, σ = 0.54 Å, and 1 kHz isotropic broadening.

Figure 3 depicts the simulated spectral fits to the experimental data. The top trace is the simulated Pake doublet for r = 1.8 Å, broadened by 15 kHz superimposed on the experimental data. The bottom trace shows the Pake doublet for R_o = 1.8 Å, σ = 0.52 Å broadened by 1 kHz also superimposed on the experimental data. Dashed lines denote the simulated spectra.

The experimental data of Fig 1 yield important clues for judicious choices of the fitting parameters. Of the three fitting parameters, the fit is most sensitive to R_o since it varies as r^{-3}. Therefore we first choose R_o according to the qualitative agreement between the unbroadened spectra and experimental data. For r = 2.4 Å, the standard result for r in SiH_2 according to theoretical calculations [2], there is a clear discrepancy in the shoulder peaks. Since subsequent broadening will only decrease the separation between peaks, it is clear that larger coupling constants (smaller r) are favored. With r = 1.8 Å, the shoulder peaks occur just outside of the experimental Pake doublet and serve as a good candidate for R_o.

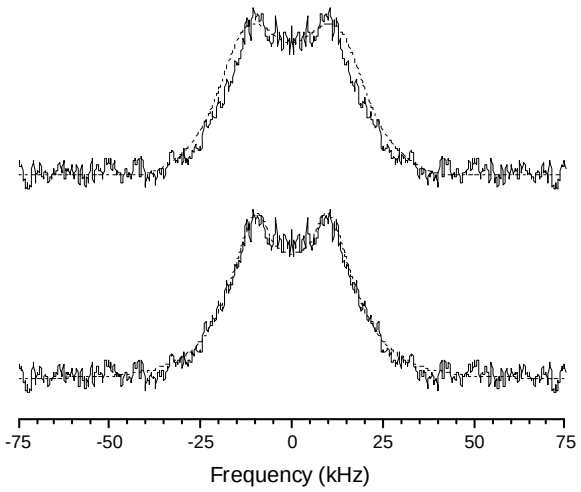

Figure 3. Simulated Pake doublets superimposed on the experimental data. The dashed line in the top trace shows the simulation fit r = 1.8 Å (no distribution) with 15 kHz isotropic broadening. The dashed line in the bottom trace shows the simulation fit for R_o = 1. 8 Å, σ = 0.54 Å, and 1 kHz isotropic broadening.

In accounting for the broadening effects, we note that the resolved peaks in the data require the total broadening to be less than the coupling constant—20.6 kHz for r = 1.8 Å. Two broadening mechanisms are available and hence any combination of the two satisfying the overall broadening requirement will yield a suitable fit. The NMR data are insufficient to answer the question of uniqueness. However, by mimicking the clustered and isolated environments known to exist for SiH (see for instance [3]), we deduce limits on the range of acceptable parameters.

We obtain the first limiting case by assuming that SiH_2 exists in hydrogen-clustered regions of the amorphous network. We also place the constraint that there exists a well-defined r = 1.8 Å for the SiH_2 sites. This seems unreasonable in light of the known nearest neighbor bond angle variation [4]. In the clustered region, the SiH_2 is isotropically broadened. The effect of 15 kHz of isotropic broadening is shown as the middle trace in Fig. 2. We present the fit to the data as the dashed line in the top trace of Fig. 3. The resulting spectrum sits outside the shoulders in the data—a discrepancy that may be accounted for by minor adjustments in R_o and the amount of isotropic broadening.

By imitating the isolated environment of SiH, we obtain the second limiting case. It is known, from hole burning experiments, that isolated SiH sees ~ 1 kHz broadening due to the surrounding hydrogen nuclei [3]. Thus we take this as our isotropic broadening parameter. To complete the broadening, we include a Gaussian distribution of *r*. The resulting spectrum with parameters R_o = 1.8 Å and σ = 0.54 Å is shown as the bottom trace of Fig. 2. The bottom trace of Fig. 3 shows the near perfect fit of these simulations to the data. Simulations with R_o = 1.9 Å and 1.7 Å have yielded inferior fits to those presented.

As demonstrated in Fig. 3 the true SiH_2 environment cannot be inferred directly from the NMR results. In either limiting case, R_o = 1.8 Å is the essential ingredient. Thus in light of prior ^{1}H NMR results linking a paired hydrogen site with *r* = 2.4 Å to the SWE, it is unlikely that an "average" SiH_2 site is involved. However, if the true *r* distribution includes this value, we cannot rule out SiH_2 as a candidate. Therefore, if the metastable, paired hydrogen site that stabilizes the SWE is indeed a SiH_2 site, then it must be a rare embodiment that is not indicative of the average site.

In summary, we have fitted the experimental Pake doublet for stable SiH_2 with line shape simulations whose fitting parameters reflect the local environment and variation in proton-proton separations. Accurate fits of the data are available for fitting parameters that imitate the clustered and isolated SiH environments. We take these sets of fitting parameters as the limiting cases whereby the true SiH_2 environment is a mixture of the two. We find for both extremes that an accurate fit is obtainable only when the proton-proton separation in SiH_2 is on average 1.8 Å. Hence a distribution of proton-proton separations is necessary if SiH_2 is to be involved with the SWE.

III. Hydrogen-Hydrogen Separation at Silicon Dihydride Bonding Sites in a-Si:H

The hydrogen bonding environments and their correlation to film quality have been the subject of an enormous body of research; see for example ref. [4]. It is generally believed that a more ordered a-Si:H matrix leads to smaller void structures and therefore to improved opto-electronic properties. As such, the concentration of large polysilane hydrogen structures, such as $(SiH_2)_n$, is thought to be small compared to the total hydrogen content for device quality films. IR studies seem to support this trend; higher quality films show no evidence of the $(SiH_2)_n$ scissor or wagging modes near 800-900 cm^{-1}. Most of the hydrogen is bonded to silicon and can be found either in clusters, such as on the internal surfaces of voids, or in isolated regions of the matrix. Since these sites occur in sufficient quantity, >1 atomic percent (at. %), they can be detected via their IR modes near 2000 cm^{-1}. Below the IR sensitivity of approximately1 at %, the hydrogen bonding structures cannot be observed, and hence the $(SiH_2)_n$ content is unknown.

We have discussed above (previous section) the ^{1}H NMR spectra of $(SiH_2)_n$ in a high defect density film. At these sites the average hydrogen-hydrogen separation is 1.8 Å [7]. In this section we describe similar $(SiH_2)_n$ structures in as-grown, higher quality material where the IR modes are absent. Of course, *n* may be unity for these sites; i.e., isolated silicon dihydride sites. Using ^{1}H NMR, which is a more sensitive probe of the bonded hydrogen, we have estimated the $(SiH_2)_n$ content for both films. We compare estimates of the $(SiH_2)_n$ content. Contrary to current

belief, we find a significant fraction of the total hydrogen content can be bonded in $(SiH_2)_n$ configurations in "device quality" films supplied by United Solar Ovonics. The film has a dark-to-photo conductivity ratio of 10^{-5}. IR absorption measurements show no evidence of the 800-900 cm^{-1} wagging or scissor modes characteristic of $(SiH_2)_n$.

The film produced at United Solar that we discussed in the previous section was intentionally grown at a high deposition rate by PECVD. As a result, a high defect density (mid 10^{17} defects cm^{-3}) film was produced that contained observable 800-900 cm^{-1} IR wagging or scissor modes. From the total intensity of these modes compared to the total 600 cm^{-1} absorption intensity due to bonded silicon monohydride, we estimate that the hydrogen occurring in the $(SiH_2)_n$ configuration is approximately 10% of the total hydrogen. It is generally accepted that the 600 cm^{-1} absorption region contains contributions from all silicon bonded hydrogen sites [8,9]. Therefore, we take 10% as an estimate of the total hydrogen bonded in the $(SiH_2)_n$ form.

The growth conditions for both films are summarized in Table 1. Results reported in this section are for the as-deposited films that have not been subjected to deliberate light soaking.

To probe the signal decay of each hydrogen component, we used the Jeener-Brockaert three-pulse sequence. Details of the pulse sequence and its utility in studying hydrogen bonding in a-Si:H can be found in ref. [10]. In this particular application, we measured the stimulated echo decay as a function of the time separation between pulse pairs. In general, the total signal amplitude, I_T, can be written as:

$$I_T(\tau_2,\tau_{1d}) = \sum_i I_{io} e^{-2\frac{\tau_2}{T_{i2}}} e^{-\left(\frac{\tau_{1d}}{T_{i1d}}\right)^{1/2}} \qquad (1)$$

where I_{io} represents the initial maximum intensity for the i^{th} component (for a discussion of the usual line shapes, see ref. [11]), T_2 is the characteristic decay time due to spin de-phasing, and T_{1d} is the dipolar spin relaxation time. Pulses 1 and 2 are separated by τ_2 (typical values are tens of μsec) while pulses 2 and 3 are separated by τ_{1d} (tens of msec typically). We determine these parameters separately by measuring the decay of the intensity as a function of τ_2 (τ_{1d}) when τ_{1d} (τ_2) is kept constant.

When the decay times are known, the total maximum intensity for each component is computed by correcting the signal intensity, at any time, with the appropriate exponential arguments given in Eq. 1. This procedure amounts to extrapolating the component signal intensity to zero time. The total signal and the relative concentrations of any component, C_i, are then computed by:

$$I_T(\tau_2 = 0, \tau_{1d} = 0) = \sum_i I_{io} \quad \text{and} \quad C_i = \frac{I_{io}}{I_T(\tau_2 = 0, \tau_{1d} = 0)} \ . \qquad (2)$$

Experimentally, it is quite difficult to obtain perfect line shape fits. The spectral features can be artificially distorted by imperfections in the detection scheme. As a result, the fits can lead to intensity mismatches that, in turn, affect the error reported in any one component. Since the measurement relies on an extrapolation of an exponential function, small uncertainties are compounded at τ_2 , $\tau_{1d} = 0$. There is also uncertainty in the total intensity incurred from the signal to noise ratio of each measurement. Our measurements are reported using the combined, additive effects of these uncertainties. This procedure yields a more conservative error estimate than the standard quadrature rules of error propagation.

Because no doublet features are observed in the NMR spectra obtained at τ_2 and $\tau_{1d} = 0$ (the free induction decay), an upper bound on the concentration of $(SiH_2)_n$ sites is estimated by calculating the total NMR frequency spectra with varying contributions from all known components. Figure 4 (bottom trace, solid line) demonstrates one such composite line shape that results when the spectra in the upper plot are added in concentrations of (top to bottom, respectively) 15%, 15% and 70%. When the percentages are 30%, 30%, and 40%, respectively, the doublet is no longer resolved. The top trace of the upper plots is a Lorentzian, corresponding to the isolated SiH and characterized by a full width at half maximum (FWHM) of 4.2 kHz. Immediately below it is a Gaussian with a FWHM of 25 kHz, which represents the clustered SiH. A simulation of the Pake doublet, where the average hydrogen-hydrogen splitting is 1.9 Å is drawn immediately below the Gaussian. This spectrum is characteristic of two strongly interacting hydrogen atoms as would occur for atoms in the $(SiH_2)_n$ configuration [7]. The percentages are representative of the minimum $(SiH_2)_n$ contribution necessary to achieve the resolved peaks near ±10 kHz shown in the bottom trace. The doublet peaks in Fig 4 help to distinguish it from the other components that mask the doublet's intensity. When these two features are present, the component concentrations can be more accurately determined.

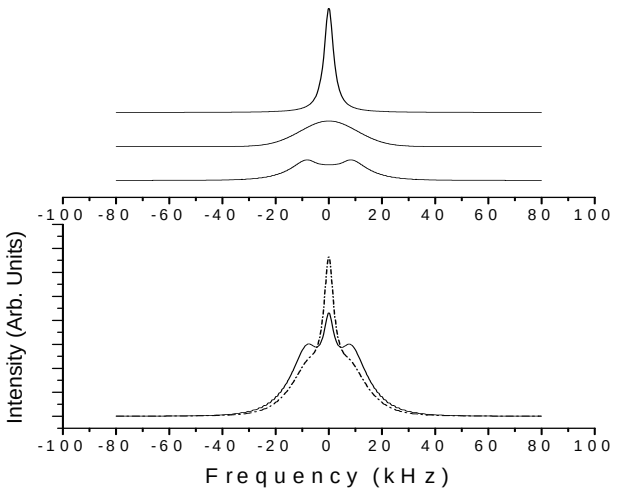

Figure 4. Estimate of the minimum ^{1}H NMR signal intensity needed to observe $(SiH_2)_n$. Top: Normalized ^{1}H NMR signals of (top to bottom) isolated SiH, clustered SiH, and $(SiH_2)_n$. Bottom: Signal resulting from addition of differing amounts of the three components. Solid line: 15% isolated SiH, 15% clustered SiH, and 70% $(SiH_2)_n$. Dashed Line: 30% isolated SiH, 30% clustered SiH, and 40% $(SiH_2)_n$

Table 1. Summary of $(SiH_2)_n$ concentration measured from NMR and IR. The reported value is the percent concentration relative to the total hydrogen concentration observable by NMR and IR. "Min %" refers to the minimum concentration estimate, within experimental uncertainty. Details of the growth conditions are also provided.

Sample	Min % $(SiH_2)_n$ NMR Estimate	% $(SiH_2)_n$ IR Estimate	Growth Conditions (films grown by PECVD)			
			Substrate Temp (^oC)	Growth Rate (Å/sec)	Power (mW/cm^2)	Pressure (mTorr)
United Solar (high quality)	12	No Modes	200	**2**	50	500
United Solar (low quality)	15	10	200	**5**	50	500

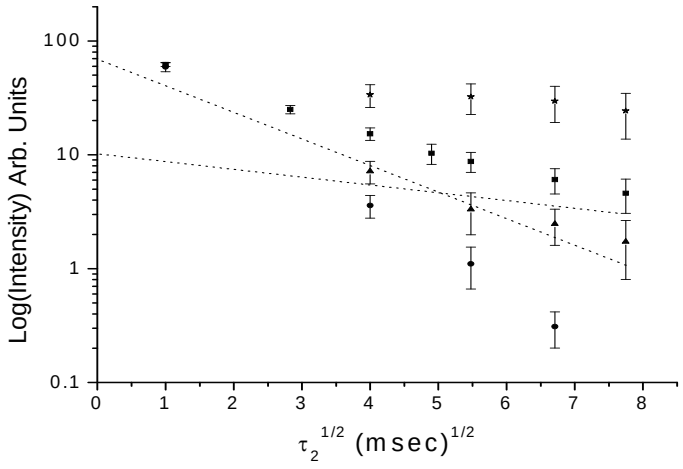

Figure 5. Log of the signal intensity as a function of $(\tau_{1d})^{1/2}$. For all data points, τ_2 = 60 μsec. "▪" represent total signal intensity, "▲" represent the $(SiH_2)_n$ intensity , "★" represent the H_2 x 10 intensity, and "●" represents the clustered and isolated SiH signal intensity. Dashed lines are aides to the eye. These two dashed lines enclose the possible $(SiH_2)_n$ signal intensities for τ_{1d} = 0 msec as allowed by experimental uncertainty.

Figure 5 shows the decay of the intensity, for the 4 components, as a function of τ_{1d} when τ_2 = 60 μsec. The data have been scaled such that the extrapolation to τ_{1d} = 0 msec is 100. The data are plotted on a log scale vs. $(\tau_{1d})^{1/2}$ so the extrapolation to τ_{1d} = 0 can be evaluated by inspection. The dashed lines, drawn as aides to the eye, enclose the τ_{1d} = 0 $(SiH_2)_n$ concentrations allowed by experimental uncertainties. The upper (lower) bound occurs near 70% (10%) of the total signal intensity. The combined Lorentzian and Gaussian contributions are plotted, since they have essentially the same T_{1d}. At τ_{1d} = 1 msec, the total Lorentzian and Gaussian components comprise essentially all of the total intensity.

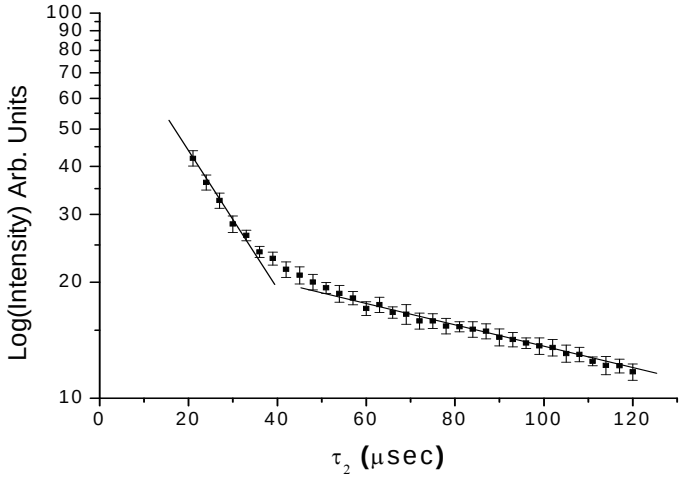

Figure 6. Log of the total signal intensity as a function of τ_2 (τ_{1d} = 1 msec for all data points) for a typical a-Si:H film. The solid lines are aides to the eye and indicate the values of T_2 for the clustered and isolated SiH. For the clustered SiH, $T_2 \cong 60$ μsec. The isolated SiH has a $T_2 \cong 300$ μsec.

Figure 6 shows the decay of the total intensity as a function of τ_2, when τ_{1d} = 1 msec for an a-Si:H sample grown under the same conditions as those listed in Table 1. The data are again scaled to read 100 at $\tau_2 = 0$ μsec. There are two distinct decay regions, as indicated by the lines. The fast (slow) decay region has $T_2 \cong 60$ μsec ($\cong 300$ μsec). These T_2 values correspond, respectively, to the Gaussian and Lorentzian components.

The data in figs. 5 and 6 are sufficient to determine the component concentrations from Eq. 2. Since T_2 is directly related to the component line width, we take 60 μsec as an approximation of T_2 for the $(SiH_2)_n$. The specific $(SiH_2)_n$ bonding environment and distribution of hydrogen-hydrogen separations is presently unknown and hence a more accurate evaluation of T_2 is unavailable. Using T_2 = 60 μsec to correct for the $\tau_{1d} = 0$ msec $(SiH_2)_n$ signal intensity, we calculate a minimum relative $(SiH_2)_n$ concentration, $C_{(SiH2)n} = 12$ %. In the same calculation, about 70 % of the total hydrogen is in the clustered configuration, 15 % exists in the isolated phase, and 1 % exists as ortho-H_2 (para-H_2 has total spin of 0 and is unobservable by NMR).

The existence of a minimum 12 % $C_{(SiH2)n}$ in the higher quality film is a bit surprising in light of the large body of NMR research on a-Si:H. However, Fig. 1 shows that $(SiH_2)_n$ must contribute a considerable fraction (~ 70 %) to the total spectrum before its features can be distinguished from the usual line shapes. If we take this as an upper bound on $C_{(SiH2)n}$, then the $(SiH_2)_n$ spectrum would not be observed by conventional free induction decay, or solid echo NMR techniques. The actual concentration of hydrogen in $(SiH_2)_n$ sites is clearly less than 70 % since no definitive evidence of $(SiH_2)_n$ from these conventional methods has been reported. As the dashed lines in Fig.1 demonstrate, the combined Gaussian and Lorentzian line shapes can mask a considerable fraction of $(SiH_2)_n$.

We have previously made similar measurements of $C_{(SiH2)n}$ in a high defect density sample of a-Si:H. The growth conditions are provided in Table 1. The NMR measurements of $C_{(SiH2)n}$ yield a range between 15 % and 60 %, consistent with $C_{(SiH2)n}$ estimates based on IR data. Within the NMR experimental error, $C_{(SiH2)n}$ can be the same for both films or, at most, differ by a factor of 6. To be consistent with the IR data for the defective film, the higher quality $C_{(SiH2)n}$ can be at most equal to the minimum detectable signal in the IR measurements. In either case, the $(SiH_2)_n$ densities differ by less than an order of magnitude in these two films.

Concentration measurements from NMR can clearly be used as a more sensitive probe of hydrogen bonding sites than the standard IR measurements. This NMR analysis will undoubtedly be useful in future film characterizations, if specific hydrogen sites are related to the metastabilities commonly observed in a-Si:H. Presently, the role of $(SiH_2)_n$ in any metastability is unclear, and a correlation between the $(SiH_2)_n$ concentration and film quality has yet to be established.

In summary, we have compared the concentration of hydrogen in $(SiH_2)_n$ sites occurring in higher quality and high defect density a-Si:H films. Our results show that, despite the large difference in film quality, the hydrogen concentrations in $(SiH_2)_n$ sites are within an order of magnitude of each other. We have shown that when compared to the usual silicon bonded hydrogen sites, 40% of the total hydrogen content can exist in $(SiH_2)_n$ structures before being visible by conventional nuclear magnetic resonance methods.

IV. Calculations of Silicon Dihydride Bonding Sites in a-Si:H

In 1977 Staebler and Wronski reported a fundamental experiment on hydrogenated amorphous silicon (a-Si:H) [12], which revealed marked decreases in both the dark and photoconductivities after light soaking. Subsequent work showed that light soaking created defects, most probably dangling bonds. Because hydrogenated amorphous silicon (a-Si:H) is a material with technological applications, understanding the phenomenon of light-induced degradation, i.e., the Staebler-Wronski effect (SWE), has been a major focus [13]. In the intervening thirty years, extensive work in experiment and modeling has been carried out to obtain the microscopic origin and fundamental understanding of light-induced degradation. Disorder in the network, hydrogen concentration and its complex bonding structure, and concentrations of impurities are some of the material properties that play a role in the SWE. We have reported an experimental clue of some importance [1] where we performed nuclear magnetic resonance (NMR) experiments on protons in a-Si:H and found that the NMR spectrum of light-soaked a-Si:H films shows the preferential creation of a hydrogen doublet where the H-H distance is 2.3 ± 0.2 Å. This experiment appears to directly connect light soaking to creation of a specific new structure (or family of structures) in the amorphous matrix. In our collaborative efforts with the group at the Ohio University, we have shown that SiH_2 is a possible candidate for the observed proton separation. Zhang, Jackson, and Chadi [14] and Chadi [15] have shown in careful calculations in c-Si:H that a two H interstitial complex, H_2^{**}, is another potential candidate for the observed defect. Both proposals have the merit that they do not rely on an unlikely conformation found only in specific models, and appear to occur with significant reproducibility, consistent with the reasonably well-defined experimental distance.

There have been various proposals for the microscopic origins of the SWE. One class of models involves breaking of "weak bonds" whose microscopic properties are often unspecified [16]. Another class of models proposes the creation of new defects as a result of movement or diffusion of an original defect [17]. Zafar and Schiff [18] considered a metastability model based upon transfer of H between clustered and isolated phases seen by NMR. Bonding in each of these phases was presumed to be monohydride. In their subsequent work Zafar and Schiff showed that the 2-phase picture closely accounted for experiments on thermal changes in the spin-density and also the changes caused by evolving hydrogen [19]. Some current theories combine the electronic and hydrogen energy states and hydrogen diffusion as in the hydrogen collision model of Branz [20], and the hydrogen flip model of Biswas and Li [21]. Kopidakis and Schiff [22] have proposed that clustered-phase sites can bind either one or two hydrogen pairs (dihydride bonding). Using this line of argument, Zhang and Branz [23] proposed a model that vacancies that produce missing Si atoms, at which the remaining Si atoms are fully terminated with Si-H bonds eliminate DB's and strained Si-Si bonds and provide the paired-H reservoir and metastability sites in a-Si:H. There are also new findings that reveal a lack of spatial correlation between the defects and hydrogen, the realization that the effectiveness of light induced defects as recombination centers depends on the light exposure conditions, and the observation that it is not only defects that are produced by extended light exposure but also larger structural changes in the material involving the Si network [13].

There are two possible interpretations of our previous NMR results [1]. The simplest interpretation is that some metastable, paired-hydrogen site, perhaps, but not necessarily SiH_2, is formed after the exposure to light. A second interpretation, which cannot be ruled out by the experiments to date, is that some changes in the various NMR relaxation rates after exposure to light allow existing paired-hydrogen sites, such as SiH_2, to become observable in the NMR spectra. Of particular importance to the latter interpretation, Stutzmann, Jackson, and Tsai [16] have argued that the breaking of weak Si-Si bonds will also promote the diffusion of dangling bonds away from their original sites. If the presence of such a dangling bond near a stable, paired-hydrogen site, for which the most logical candidate is SiH_2, allows this site to be seen in the H NMR, then the results of Su et al. are also logically explained. Although there are technical reasons why this explanation is not as probable as the formation of metastable, paired-hydrogen sites, it cannot be ruled out. The simulations in collaboration with the Ohio University group support either of these two interpretations.

In these simulations we used the *ab initio* code, SIESTA [24,25,26], within the local density approximation (LDA). Details of these simulations are available elsewhere [27].

The calculations began with a defect-free 64-atom a-Si model [28] and removed two Si atoms and added 8 H atoms to create defect-free (that is, gap state free) structures with SiH_2 present. This model is denoted as aSiH-70. Another model is obtained in the same way except that one more Si atom is removed to form aSiH-72 (61 Si atoms and 11 H atoms), which includes one dangling bond [29]. This supercell surgery was repeated at other sites to generate an ensemble of models to obtain some insight into the bonding statistics of SiH_2 conformations in the solid state. The SiH_2 confirmations obtained in the two models are shown in Fig. 7(a) and

Fig. 7(b). Four configurations were considered for each model in our calculation. Each configuration in the respective models was constructed by selecting different (typically tetrahedral) sites of the SiH_2 conformations in the cell. Calculations of the SiH_2 structures and dynamics on each of the four configurations of the aSiH-70 model and also on each of the four configurations of the aSiH-72 model were performed. The system was then relaxed. Details of the relaxation procedures are available elsewhere [27]. There is a consistent pattern that in the amorphous matrix the proton-proton separation is significantly reduced relative to a gas phase silane molecule with tetrahedral bonds (which produces a separation of 2.45 Å).

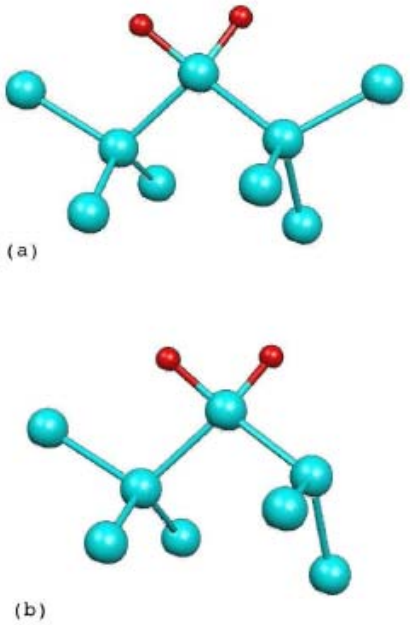

Figure 7. (a) SiH2 conformation in aSiH-70 model and (b) SiH2 conformation in aSiH-72 model with a dangling bond. In the figure the hydrogen atoms are shown in red (smaller in size) and the silicon atoms are shown in cyan (larger in size).

Thermal molecular dynamics (MD) simulations were performed to estimate the H-H distance at room temperature and to compare to T=0. The cells evolved freely for 250 fs (within a time step of 0.05 fs) at a temperature of T = 300 K. Thermal fluctuations in the bond lengths were observed as indicated in Fig. 8(a), and from Fig. 8(b). Over 5000 step MD runs, the average H-H distance becomes 2.41 Å in the case of the LDA calculations and 2.34 Å for the GGA calculations for an initial H-H distance of 2.27 Å.

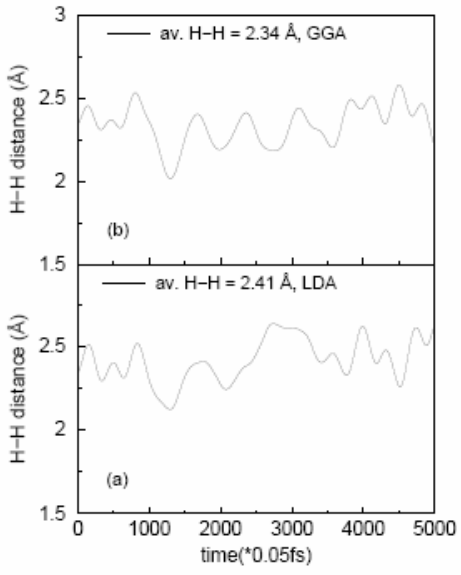

Figure 8. Thermal MD simulation for the H-H distance in aSiH-72 model using a) LDA calculations and b) GGA calculations [21].

The same calculation has also been done for the aSiH-72 model. Consistent with the first configuration, the aSiH-72 model also gives proton separations well within the tolerance of the experiments of Su et al. [1].

Most of the aforementioned models of the SWE invoke paired-hydrogen sites. These models associate the SWE with the conversion of isolated H into paired-hydrogen sites, for which SiH_2 must be considered a prime candidate. The experiments of Su et al. [1] provide direct evidence that light soaking creates structures with a proton-proton separation of about 2.3 Å. Given the remarkably well-defined nature of the observed proton separation, it is natural to expect that the structure(s) causing the feature must not be a very rare conformation. Something like the complex of Chadi [15], or the SiH_2 proposal presented here, appear to fulfill that condition – one certainly expects a priori that both of these configurations should occur in a-Si:H, although it is not initially obvious with what probability.

Given that the various models proposed [9−23] all appear to be at least consistent with our calculations for SiH_2, the link between these calculations and the NMR experiments could be a very important step. On the other hand, what has not been done is to provide any explanation of the light-induced formation of SiH_2, which is certainly a key missing piece to the puzzle. This is not an easy process to simulate, since the (diffusive) time-scales for creation are presumably vastly longer than what is directly accessible from our simulation.

In summary, using accurate methods and supercells properly representing the disorder of a-Si:H, we have seen that SiH_2 is a credible candidate for the proton-proton distance inferred from the work of Su et al. [1]. The results indicate clearly that rather accurate methods are needed to properly describe the bonding in this system.

V. Additional Research Efforts

In addition to our extensive collaborative studies with United Solar Ovonics on samples that contain large densities of silicon dihydride bonding sites and on defects that contribute to the Staebler-Wronski effect, we are completing our collaborative studies with NREL on tritiated samples and on light soaking of samples at 77 K. We hope eventually to perform measurements on a-Ge:H in collaboration with United Solar Ovonics, but our experiments so far have shown that the defect densities are too high to perform the light soaking experiments. If these experiments are eventually successful, we will plan the NMR measurements on large-area samples. Finally, we have initiated a new set of experiments in collaboration with United Solar Ovonics and MVSystems on defects, metastabilities, and hydrogen bonding sites in nanocrystalline Si that may eventually replace the bottom cell in tandem devices.

VI. Summary

During Phase II of the current sub-contract we have made significant progress in understanding the role of SiH_2 in both high and low defect-density films of a-Si:H. We have also calculated the H-H separation at SiH_2 sites that may be consistent with that observed in NMR light-soaking experiments.

REFERENCES

1. T. Su, P.C. Taylor, G. Ganguly, and D.E. Carlson, Phys. Rev. Lett. 89, 015502 (2002).
2. Tesfaye A. Abtew, D. A. Drabold, and P. C. Taylor, Appl. Phys. Lett. 86, 241916 (2005).
3. J. A. Reimer, R. W. Vaughn, and J.C. Knights, Phys. Rev. B 24, 3360 (1981).
4. R. A. Street, *Hydrogenated Amorphous Silicon,* Cambridge University Press, Cambridge, England, (1991).
5. C. P. Slichter, *Principles of Magnetic Resonance*, Springer Series in Solid-State Sciences, Springer Verlag, 3rd enlarged and updated ed., Jan. (1990).
6. S.A. Smith, T.O. Levante, B.H. Meier, and R.R. Ernst, *J. Magn. Reson.*, **106a**, 75-105, (1994).
7. D. C. Bobela, T. Su, P. C. Taylor and G. Ganguly, J. Non. Cryst. Sol., 2006, *in press*.
8. M. H Brodsky, Manuel Cardona, and J. J. Cuomo, Phys. Rev. B **16**, 3556 (1977).
9. W. B. Pollard, and G. Lucovsky, Phys. Rev. B **26**, 3172 (1982).
10. T. Su, S. Chen, and P. C. Taylor, Phys. Rev. B **62**, 12849 (2000).
11. W. E. Carlos, and P. C. Taylor, Phys. Rev. B **26**, 3605 (1982).
12. D. L. Staebler and C. R. Wronski, Appl. Phys. Lett. **31**, 292 (1977).
13. H. Fritzsche, Annu. Rev. Mater. Res. **31** 47-79 (2001).
14. S. B. Zhang, W. B. Jackson and D. J. Chadi, Phys. Rev. Lett. **65** 2575 (1990).
15. D. J. Chadi, App. Phys. Lett. **83** 3710 (2003).
16. M. Stutzmann W. B. Jackson and C. C. Tsai, Phys. Rev. **B 32** 23 (1985).
17. R. Biswas, I. Kwon and C. M. Soukoulis, Phys. Rev. **B 44** 3403 (1991).
18. S. Zafar and E. A. Schiff, Phys. Rev. **B 40** 5235 (1989);
19. S. Zafar and E. A. Schiff, Phys. Rev. Lett. **66** 1493 (1991); ibid. J. Non-Cryst. Sol. 137-138 323 (1991).
20. H. M. Branz, Phys. Rev. **B 59** 5498 (1999).
21. R. Biswas and Y. -P. Li, Phys. Rev. Lett. **82** 2512 (1999).
22. N. Kopidakis and E. A. Schiff, J. Non-Cryst. Sol. **266-269** 415 (2000).
23. S. B. Zhang and Howard M. Branz, Phys. Rev. Lett. **87** 105503 (2001); for a recent review see H. Branz, Solar Energy Materials and Solar Cells **78** 425 (2003).
24. P. Ordej´on, E. Artacho and J. M. Soler, Phys. Rev. **B 53** 10441(1996).
25. D. S´anchez-Portal, P. Ordej´on, E. Artacho and J. M. Soler, Int. J. Quantum Chem. **65** 453 (1997).
26. J. M. Soler, E. Artacho, J. D. Gale, A. Garc´ıa, J. Junquera, P. Ordej´on and D. S´anchez-Portal, J. Phys.: Condens. Matter **14** 2745 (2002).
27. T. A. Abtew, D. A. Drabold, and P. C. Taylor, Appl. Phys. Lett. **86**, 241916-1 (2005).
28. G. T. Barkema and N. Mousseau, Phys. Rev. **B 62** 4985 (2000).
29. This second conformation reveals only that the proton-proton distances reported are “robust” even for a rather different chemical environment. It is unlikely that the SiH2 would be so close to a dangling bond. See S. Yamasaki, H. Okushi, A. Matsuda, K. Tanaka and J. Isoya, Phys. Rev. Lett. **65** 756 (1990).